Published in final edited form as:
J Am Chem Soc. 2005 August 10; 127(31): 11075–11084. doi:10.1021/ja0522027.

In Vitro Characterization of Salmochelin and Enterobactin Trilactone Hydrolases IroD, IroE, and Fes

Hening Lin[†], **Michael A. Fischbach**[†,‡], **David R. Liu**[‡], and **Christopher T. Walsh**[†,*]

† *Department of Biological Chemistry & Molecular Pharmacology, Harvard Medical School, Boston MA 02115*

‡ *Department of Chemistry & Chemical Biology, Harvard University, Cambridge, MA 02138*

Abstract

The *iroA* locus encodes five genes (*iroB*, *iroC*, *iroD*, *iroE*, *iroN*) that are found in pathogenic *Salmonella* and *Escherichia coli* strains. We recently reported that IroB is an enterobactin (Ent) C-glucosyltransferase, converting the siderophore into mono-, di- and triglucosyl enterobactins (MGE, DGE, and TGE, respectively). Here we report the characterization of IroD and IroE as esterases for the *apo* and Fe^{3+}-bound forms of Ent, MGE, DGE, and TGE, and we compare their activities with those of Fes, the previously characterized enterobactin esterase. IroD hydrolyzes both *apo* and Fe^{3+}-bound siderophores distributively to generate DHB-Ser and/or Glc-DHB-Ser, with higher catalytic efficiencies (k_{cat}/K_m) on Fe^{3+}-bound forms, suggesting that IroD is the ferric MGE/DGE esterase responsible for cytoplasmic iron release. Similarly, Fes hydrolyzes ferric Ent more efficiently than *apo* Ent, confirming Fes is the ferric Ent esterase responsible for Fe^{3+} release from ferric Ent. Although each enzyme exhibits lower k_{cat}'s processing ferric siderophores, dramatic decreases in K_m's for ferric siderophores result in increased catalytic efficiencies. The inability of Fes to efficiently hydrolyze ferric MGE, ferric DGE, or ferric TGE explains the requirement for IroD in the *iroA* cluster. IroE, in contrast, prefers *apo* siderophores as substrates, and tends to hydrolyze the trilactone just once to produce linearized trimers. These data and the periplasmic location of IroE suggest that it hydrolyzes *apo* enterobactins while they are being exported. IroD hydrolyzes *apo* MGE (and DGE) regioselectively to give a single linear trimer product and a single linear dimer product as determined by NMR.

Introduction

Iron is an essential cofactor for most bacterial species.[1] The iron supply is normally limited in the environment because of the low solubility of Fe^{3+} at neutral or basic pH. In mammalian hosts, the free Fe^{3+} concentration is further lowered by Fe^{3+}-binding proteins to an estimated 10^{-24} M.[1] To survive in an iron-deficient environment, bacteria have evolved the ability to biosynthesize dedicated Fe^{3+}-binding small molecules, or siderophores, to scavenge iron from the environment.[2] One of the best studied siderophores is enterobactin (Ent) (Figure 1), a 2,3-dihydroxybenzoylserine macro-trilactone produced by enteric bacteria such as *E. coli* and *Salmonella enterica*.[1] Ent is the strongest Fe^{3+} ligand known with an estimated K_D of 10^{-49} M (10^{-35} M at physiological pH).[3,4] The genes involved in the biosynthesis, transport, and processing of Ent are clustered into a 20 kB region of the bacterial chromosome controlled by the iron-dependent repressor Fur.[2] The biosynthesis of Ent from 2,3-dihydroxybenzoic acid (DHB) and Ser requires the action of EntB, EntD, EntE and EntF[5–8] and follows nonribosomal peptide synthetase logic.[2,9] Following synthesis in the bacterial cytoplasm, Ent is exported

*To whom correspondence should be addressed. E-mail: christopher_walsh@hms.harvard.edu.

from the cell in a process that involves YbdA (EntS).[10] Ent molecules that have successfully bound to extracellular Fe^{3+} are recognized by the outer membrane receptor FepA and are imported through an active transport process.[11,12] Iron release from Fe-Ent requires the enzyme Fes, which has been shown to catalyze the hydrolysis of Fe-Ent despite conflicting reports on whether Fes prefers *apo* Ent or Fe-Ent as substrate.[13–16] Since the DHB-Ser monomer has a much lower affinity for Fe^{3+}, the hydrolysis event facilitates the transfer of Fe^{3+} to iron-dependent enzymes such as cytochromes.

Recently, C-glucosylated Ent analogs, termed salmochelins, have been isolated from *S. enterica* and structurally characterized.[17,18] Salmochelin production could be a mechanism by which pathogenic bacteria subvert a mammalian host's innate immunity. One observation that supports this is that salmochelins are better siderophores than Ent in the presence of serum albumin.[17] Another observation is that ferric Ent is sequestered by the protein siderocalin in a mammalian host,[19,20] and glucosylation of Ent presumably decreases the affinity for siderocalin. The conversion of Ent to salmochelins such as S1, S2, and S4 (Figure 1), requires the *iroA* gene cluster, which includes five genes, *iroB*, *iroC*, *iroD*, *iroE* and *iroN*.[21] The IroN protein has homology to FepA and was shown to be an outer membrane receptor for uptake of Fe^{3+}-bound salmochelins.[18,21] Similar to FepA and Cir, IroN is also able to recognize several other siderophores.[22] IroC is thought to be an inner membrane transporter, functioning in the export of *apo* siderophores.[23] IroB has been shown to catalyze the C-glucosylation of Ent.[17,23] The two remaining proteins, IroD and IroE, are homologous to Fes. IroD has been predicted to be cytoplasmic while IroE is thought to be periplasmic.[18] Bacterial strains that harbor an *iroA* cluster lacking IroD or IroE produce less of the hydrolyzed salmochelins (S1, S2, and SX), suggesting that both enzymes are probably salmochelin esterases.[17,23] It is not clear why two esterases are present in the *iroA* cluster, how they differ in catalytic efficiency and specificity, or if Fes is able to release Fe^{3+} from salmochelins. These questions are the subject of the work reported herein.

We recently purified and characterized the proposed glucosyltransferase (Gtf) IroB[24] and established that it can catalyze the successive mono-, di- and tri-C-glucosylation of Ent to generate monoglucosyl enterobactin (MGE), diglucosyl enterobactin (DGE), and triglucosyl enterobactin (TGE) (Figure 1). DGE is identical to salmochelin S4, while S1, S2, and SX correspond to MGE and DGE hydrolysis products that may rise from the action of IroD or IroE. The availability of pure, active IroB [24] enables the preparation of sufficient MGE, DGE, and TGE to assay the enzymatic properties of IroD and IroE for both catalytic efficiency and regioselectivity of cleavage. We also compare the kinetic parameters of these two enzymes with those of Fes.

Materials and Methods

Preparation of Ent and glucosylated Ents

Ent was chemically synthesized as reported previously.[24,25] The enzymatic synthesis of TGE was described previously.[24] For the synthesis of MGE and DGE, a slightly modified method was used. To 150 mL Tris buffer (75 mM, pH 8.0) containing $MgCl_2$ (5 mM), tris(2-carboxyethyl)phosphine (2.5 mM), UDP-Glc (1.5 mM), and Ent (1 mM), was added IroB to a final concentration of 56 mg/L. The reaction was gently agitated at 23°C for 2 hrs, then quenched with 50 mL 2.5 N HCl in methanol. After filtering through a 0.45 μm membrane, the MGE and DGE products were purified by reverse phase HPLC using a gradient of 0–40% CH_3CN in 0.1% TFA/water over 40 min. Fractions containing MGE and DGE were lyophilized to give the products as white solids (~50 mg each). All compounds in apo forms were dissolve in DMSO to be used in enzyme assays.

Preparation of ferric complexes of Ent, MGE, DGE, and TGE

Since previous inconsistency on Fes substrate specificities were attributed to possible differences in the Fe-Ent samples, we tried two methods to prepare the ferric complex. (**A**) Ent, MGE, DGE, or TGE (6.4 mM in DMSO) was mixed with 1.2 equivalent of $FeCl_3$ (6.4 mM in water) for 2 min at 23°C. To the colored solution was then added 75 mM HEPES buffer (pH 7.5) to make the final ferric complex concentration 128 μM. This solution was then left at 23°C for at least 1 hr before being used in enzyme assays. (**B**) Ent, MGE, DGE, or TGE (6.4 mM in DMSO, 200 μL) was mixed with 1.1 equivalent of $FeCl_3$ (6.4 mM in water, 220 μL) and 3.3 eq of 1M aqueous K_2CO_3 (4.2 μL) for 1 min at 23°C. The colored solution was then loaded onto an anion exchange column packed with 10 mL DEAE Sephacel resin (Amersham). After washing with 3 column volumes of water, 3 column volumes of 0.1 M NaCl, the ferric complex was eluted with 2–4 column volumes of 1 M NaCl or a gradient of NaCl. To the pink solution containing the ferric complex was added 4 volumes of ethanol. The salt precipitate was removed by centrifugation, and the supernatant was concentrated by rotary evaporation. The residue was then re-suspended in 80% ethanol (10 mL), and insoluble salt again was removed by centrifugation, and the supernatant was concentrated by rotary evaporation. The final residue was re-suspended in 80% ethanol (0.5 mL), and any salt precipitation was removed by centrifugation. The ferric complex, by dissociation with HCl and HPLC analysis monitored at 316 nm and 220 nm, contained more than 95% intact macrolactone scaffold and only very little side product. The concentration of the ferric complex solution was determined by comparing the area of absorption in the HPLC trace with that of a known concentration *apo* Ent solution. The solution was then diluted with 75 mM HEPES pH 7.5 buffer to make the final concentration 128 μM. The ferric siderophore solution thus obtained was checked with UV-Vis spectroscopy and compared with the spectrum of the *apo* compound. The *apo* form has an absorption at 320 nm, while the ferric form has absorptions at 340 nm and 496 nm, consistent with literature for Ent and Fe-Ent[3,26]. We carried out enzyme assays with ferric complexes prepared by both methods and found they behaved essentially the same. The kinetic data presented in the result section were obtained with ferric complexes prepared by method B.

Cloning, expression, and purification of IroD

The *iroB* gene was amplified from *E. coli* CFT073 genomic DNA using the forward primer 5′-ggaattccatatgctgaacatgcaacaacatc-3′ and the reverse primers 5′-gatcgaattctcaaccctgtagtaaaccaatcccg-3′ (pET-28b) and 5′-gatcgaattcggaccctgtagtaaaccaatcccgtc-3′ (pET-22b). The forward primer introduced an *Nde*I restriction site and the reverse primers introduced *EcoR*I restriction sites (underlined above). PCR reactions were performed with Herculase DNA polymerase (Stratagene). The amplified gene sequences were digested with *Nde*I and *EcoR*I (New England Biolabs), then ligated into the expression vectors pET-28b and pET-22b, and transformed into *E. coli* TOP10 cells (Stratagene). The identities of the resulting pET-28b-IroD (N-His) and pET-22b-IroD (C-His) constructs were confirmed by DNA sequencing. Expression constructs were transformed into *E. coli* BL21(DE3) cells, grown to saturation in LB medium supplemented with kanamycin (50 μg/ml) or ampicillin (100μg/ml) at 37 °C, and diluted 1:100 into LB medium supplemented with kanamycin (30 μg/ml) or ampicillin (50μg/ml). The expression of N- and C-terminal His_6 fusion proteins was induced at OD_{600} 0.5–0.6 with 400 μM IPTG and overexpression was allowed to proceed at 15 °C for 20 h. Cells from 2 L cultures were pelleted by centrifugation (10 min at 6100 *g*), resuspended in 15 ml Buffer A (20 mM Tris pH 8.0, 500 mM NaCl, 10 mM $MgCl_2$, 5 mM imidazole), and lysed by two passages through a cell disruptor (Avestin EmulsiFlex-C5) at 5000–15000 psi. Cell debris was removed by ultracentrifugation (30 min at 126000 *g*), and the supernatant was incubated with 1 mL Ni-NTA resin (Qiagen) at 4 °C for 2 h. After discarding the unbound fraction, the resin was resuspended in 3 ml Buffer A, loaded onto a column, and washed with 10 mL Buffer A. IroD was eluted from the column with a

stepwise imidazole gradient (from 10 mM to 200 mM). After SDS-PAGE analysis, fractions containing pure IroD were pooled and dialyzed twice against 2 L Buffer B (25 mM Tris pH 8.0, 50 mM NaCl, 1 mM DTT, 10% (v/v) glycerol). The protein was flash-frozen in liquid N_2 and stored at −80 °C. The concentrations of purified IroD N-His_6 and C-His_6 were determined spectrophotometrically at 280 nm using calculated extinction coefficients of 72030 M^{-1} cm^{-1} for both proteins.

Cloning, expression, and purification of IroE N-30

IroE N-30 trunction was PCR amplified from *E. coli* CFT073 genomic DNA using the forward primer 5′-ggaattccatatgtatgcgaagccggatatgcg-3′, and reverse primer 5′-gatcgaattcgggtggcttaactcatgacaacctgc-3′, digested and ligated into pET-22b. The expression and purification followed the same procedure as described for IroD. The concentration of purified IroE N-30 C-His_6 were determined spectrophotometrically at 280 nm using calculated extinction coefficient of 45041 M^{-1} cm^{-1}.

Cloning, expression, and purification of Fes N-His

Fes was PCR amplified from *E. coli* CFT073 genomic DNA using the forward primer 5′-ggaattccatatgtttgaggtcactttctggtg-3′, and reverse primer 5′-gatcgaattctcaactcctgtcatggaaaagtg-3′, digested and ligated into pET-28b. The expression in BL21(DE3) cells were carried out at 15 °C for 3 days with 4 L culture and no IPTG induction. Unless otherwise noted, the same procedure as described for IroD was followed. The fractions containing impure Fes from the Ni-NTA purification were pooled and further purified by FPLC with a Superdex 200 (Amersham) gel filtration column and a MonoQ 10/100 GL (Amersham) anion exchange column at 4°C. After SDS/PAGE analysis, the fraction containing the relatively pure Fes protein was concentrated using Amicon Ultra centrifugation filter devices (Millipore), dialyzed, flash frozen with liquid N_2, and stored at −80°C. The concentration of purified Fes N-His_6 were determined spectrophotometrically at 280 nm using calculated extinction coefficient of 124704 M^{-1} cm^{-1}.

Initial enzyme activity assay with *apo* Ent, MGE, DGE, and TGE

For the initial activity assay with *apo* siderophores, all reactions were carried out in 75 mM HEPES buffer pH 7.5 with 32 μM substrates. IroD, IroE and Fes frozen stocks were thawed on ice, diluted to 1 μM with cold buffer B, and then added to the reaction mixture to a final concentration of 20 nM. The reactions were quenched with 0.5 volumes of 2.5 N HCl in methanol and analyzed by LCMS with a gradient of 0–35% CH_3CN (with 0.1% formic acid) in water (with 0.1% formic acid) over 8 min. The MS m/z data for different substrates and hydrolysis product are listed in Table 1.

Initial enzyme activity assay with ferric Ent, MGE, DGE, and TGE

For the initial activity assay with ferric siderophores, reaction conditions were the same as for *apo* siderophores, except that the siderophores were mixed with 1.2 eq of $FeCl_3$ in the reaction buffer for 10 min before the addition of enzymes.

Enzyme kinetics with *apo* Ent, MGE, DGE, TGE

All reactions were carried out in duplicate in 200 μL 75 mM HEPES buffer pH 7.5 at 23 °C, with substrate concentrations ranging from 2 μM to 128 μM or 256 μM. Reactions were quenched with 100 μL 2.5 N HCl in methanol, and then frozen on dry ice. For HPLC analysis, the samples were thawed just before injection. Product quantification was based on the area of absorption monitored at 316 nm, assuming hydrolysis of the ester bond does not affect the absorption. Negative control reactions without enzyme were also carried out so that the background hydrolysis could be subtracted from the data. For IroE, the enzyme concentration

used was 20 nM, and reactions were quenched after 40 sec. For IroD, the enzyme concentration used was 5 nM, and reactions were also quenched after 40 sec. For Fes, 27 nM enzyme was used for Ent and MGE hydrolysis, and reactions were quenched after 40 sec; 36 nM enzyme was used for DGE hydrolysis, and reactions were quenched after 5 min.

Enzyme kinetics with ferric Ent, MGE, DGE, TGE

Unless otherwise noted, reaction conditions were the identical to those involving *apo* Ent, MGE, DGE, and TGE. The ferric siderophores were prepared using method B. The substrate concentrations used in the assays ranged from 0.125 μM to 16 μM. For IroE, the enzyme concentration used was 320 nM, and reactions were quenched after 2min for Fe-Ent, Fe-MGE, and Fe-DGE, 1 min for Fe-TGE. For IroD, the enzyme concentration used was 5 nM, and reactions were quenched after 40 sec. For Fes, consistent with previous report,[16] we found DTT and $MgCl_2$ increased the hydrolysis rate several fold. Therefore, all reactions with Fes were carried out with 2 mM DTT and 2 mM $MgCl_2$. The Fes concentration used was 14 nM for Fe-Ent hydrolysis, and reactions were quenched after 40 sec; 36 nM for Fe-MGE hydrolysis, and reactions were quenched after 3 min.

Preparation of MGE and DGE hydrolysis products for NMR characterization

To 150 mL HEPES buffer (75 mM, pH 7.5) containing MGE or DGE (250 μM) was added IroD C-His_6 (2 μM, 6 mL) to a final concentration of 80 nM. The reaction was gently agitated at 23°C for 2 min (MGE) or 1.5 min (DGE) and then quickly quenched with 50 mL 2.5 N HCl in methanol. The hydrolysis products were purified by HPLC using a gradient of 0–40% CH_3CN in 0.1% TFA/water over 40min. The major product obtained this way was the linear trimer. By extending the reaction time to 4 min, the major product obtained was the linear dimer. The linear trimers and dimers from MGE and DGE hydrolysis were dissolved in methanol-d_4 and the NMR experiments (^1H, ^{13}C, COSY, HSQC, HMBC) were done using Varian 500 MHz NMR spectrometer in the Chemistry and Chemical Biology Department of Harvard University. The spectra can be found in the supporting information.

Results

Overexpression and Purification of IroD, IroE, and Fes

The *iroD*, *iroE* and *fes* genes were cloned from *E. coli* CFT073 into *E. coli* protein expression vectors as N-terminal or C-terminal His_6 fusions. IroD (410 aa, 45 kDa) was overexpressed from *E. coli* BL21/DE3 cells and purified by Ni-NTA affinity purification to > 95% purity (Figure 2).

In contrast, IroE (318 aa, 35 kDa), the predicted periplasmic protein, was insoluble under similar overexpression conditions. Hydropathy analysis (http://www.predictprotein.org) predicted that residues 20–30 form a transmembrane region. We hypothesized that deletion of the transmembrane region might increase the solubility of the resulting truncated IroE protein. Therefore, genes encoding IroE variants lacking the first 10, 20, 30, or 40 residues were constructed and the corresponding proteins were overexpressed. Deletion of the first 10 or 20 amino acids still yielded insoluble proteins, but deletion of the first 30 or 40 amino acids (N-30, N-40) generated soluble proteins that could be purified to > 95% purity (Figure 2). Initial enzyme activity assays with Ent and MGE showed that both the N-30 and N-40 truncations of IroE were active. Subsequent kinetic studies were carried out with the N-30 truncation, containing residues 31–318 of IroE.

The expression and purification of Fes (374 aa, 43 kDa), previously characterized by Brickman and MacIntosh,[16] proved to be challenging. Fes was not soluble under conditions used for IroD overexpression and purification. Unlike IroE, N-terminal truncation did not remedy this

insolubility. Sufficient soluble Fes was obtained in roughly 50% purity by limiting expression of Fes to the background level resulting from the absence of IPTG in the growth media. During anion exchange and gel filtration purification steps, the Fes protein co-purified with two other proteins, suggesting the possibility of a tight physical association with these proteins. One chromatographic fraction contained Fes in ~ 90% purity; assays with Fes were conducted using this fraction (Figure 2).

Initial enzyme activity assay of IroD, IroE, and Fes with *apo* substrates

Initial studies were performed with the *apo* siderophores. Ent was chemically synthesized as previously reported [25] while MGE, DGE, or TGE were synthesized enzymatically with IroB from Ent and UDP-Glc.[24] Although TGE was not isolated from *iroA*-harboring bacterial strains and may not be physiologically relevant, we included TGE in our assays.

Activity assays of IroE were carried out at pH 7.5 with 20 nM IroE and 32 μM Ent, MGE, DGE, or TGE. Reactions were monitored by LC/MS. The time courses of the IroE catalyzed hydrolysis reactions shown in Figure 3 indicate that (i) Ent, MGE, DGE and TGE are all substrates of IroE, but Ent and MGE seem to be hydrolyzed faster than DGE and TGE. This trend can also be seen from the catalytic efficiency values shown in Table II below; (ii) the initial linear trimer products of trilactone hydrolysis are not efficient substrates for further hydrolysis, enabling the reaction to stop at the linear trimer stage; (iii) IroE acts with little regioselectivity relative to the placement of the C-glucosyl substituent on the trilatone, since at least two closely eluting product peaks (separable upon analytical HPLC analysis) were observed with the same mass for MGE and DGE hydrolysis. Due to the difficulty in separating these products, we did not further pursue their structural characterization, unlike the IroD case described below.

The activity assays of IroD were carried out in a similar manner. The assay results shown in Figure 3 are consistent with three conclusions: (i) *apo* Ent, MGE, DGE, and TGE are all substrates for hydrolysis by IroD; (ii) the initial linear trimer products are in turn very good substrates for further hydrolytic cleavage by IroD, leading to complete degradation of the trilactone to DHB-Ser and/or Glc-DHB-Ser monomers; (iii) only one isomer of the linear trimer product and one isomer of the linear dimer product from MGE or DGE hydrolysis were observed, suggesting that IroD hydrolyzes MGE and DGE regioselectively. Interestingly, the linear dimer products from MGE and DGE hydrolysis both have a molecular weight of 627 Da, indicating the presence of a single glucose group in both dimers.

Under similar assay conditions, we found that *E. coli* Fes catalyzes the hydrolysis of *apo* Ent and *apo* MGE, but catalyzes the hydrolysis of *apo* DGE very poorly, and does not process *apo* TGE at all (Figure 3). These results indicate that Fes exhibits a bias against processing the more extensively glucosylated trilactone substrates.

Initial enzyme activity assay of IroD, IroE, and Fes with Fe-Ent, Fe-MGE, Fe-DGE, and Fe-TGE

Release of iron from Fe-Ent molecules imported to the cytoplasm is thought to occur by Fes-catalyzed hydrolysis of the trilactone scaffold of Fe-Ent.[1] By analogy, iron release from glucosylated Ent following import to the bacterial cell could be achieved by IroD- and/or IroE-catalyzed hydrolysis. However, previous studies on Fes reached disparate conclusions about its preference for *apo* or Fe^{3+}-bound Ent as substrate,[13,14,15,16] with several reports suggesting that Fes preferentially hydrolyzes *apo* Ent. We therefore tested whether IroD and IroE can catalyze the hydrolysis of Fe^{3+}-bound siderophores (Figure 4). To our surprise, we found that under conditions similar to those for the *apo* siderophore hydrolysis assays, IroE hydrolyzes the Fe^{3+}-bound siderophores very inefficiently. IroD catalyzes the hydrolysis of Fe^{3+}-bound siderophores, with rates faster than those of IroE for ferric substrates, but about

100-fold lower than those of IroD for *apo* substrates. We also examined the hydrolysis of Fe-Ent by Fes with the purified Fes protein and found that the rate is also about 100-fold slower for Fe-Ent than for *apo* Ent. The reluctance of Fes, IroD, and IroE to hydrolyze Fe^{3+}-bound siderophores seemed at odds with their presumed physiological function of releasing bound Fe^{3+}. The detailed kinetics studies described below resolved this apparent contradiction.

Kinetic parameters of Fes, IroD and IroE

The kinetic parameters of Fes-, IroD- and IroE-catalyzed hydrolysis of both *apo* and Fe^{3+}-bound forms of Ent, MGE, DGE, and TGE were measured and are summarized in Table 2.

For Fes-catalyzed *apo* Ent hydrolysis, no saturation was observed at Ent concentrations up to 128 μM, arguing against the *apo* form as natural substrate. We observed that k_{cat}/K_m = 4.0 $\mu M^{-1}min^{-1}$, K_m is greater than 128 μM and therefore inferred that k_{cat} is greater than 512 min^{-1}. In contrast, for Fes-catalyzed Fe-Ent hydrolysis, the reaction reaches saturation even at 0.125 μM Fe-Ent concentration, which was the lowest concentration tested given the sensitivity limit of the HPLC assay used. We determined the k_{cat} of Fes on Fe-Ent to be 9 min^{-1}, K_m to be less than 0.1 μM, and therefore inferred that k_{cat}/K_m is greater than 90 $\mu M^{-1}min^{-1}$. The decrease in k_{cat} for Fes-catalyzed hydrolysis of Fe-Ent versus *apo* Ent explains why we observed a much slower reaction for Fe-Ent hydrolysis in the initial enzyme assays. However, the catalytic efficiency (k_{cat}/K_m) of Fes for processing Fe-Ent is much higher than that for *apo* Ent, suggesting that Fe-Ent is the physiological substrate of Fes.

Fes catalyzes the hydrolysis of Fe-MGE, albeit 20-fold less efficiently than Fe-Ent, but does not catalyze the hydrolysis of Fe-DGE or Fe-TGE. The catalytic efficiency of Fes for Fe-MGE is very small compared to the catalytic efficiency of Fes for Fe-Ent, or the catalytic efficiency of IroD for Fe-MGE and Fe-DGE. Therefore, Fes is unlikely to be the enzyme that hydrolyzes Fe-MGE or Fe-DGE to release Fe^{3+}, explaining the need for a separate salmochelin hydrolase.

IroD catalyzes the hydrolysis of both the *apo* and Fe^{3+}-bound forms of Ent, MGE, DGE, and TGE. Furthermore, we observed a k_{cat}/K_m preference for the Fe^{3+}-bound form of Ent, MGE, DGE, and TGE over the *apo* forms. Both k_{cat}'s and K_m's are smaller for the Fe^{3+}-bound forms than the *apo* forms, but the decreases in K_m's are more dramatic, resulting in higher k_{cat}/K_m values for the Fe^{3+}-bound form.

IroE also hydrolyzes both *apo* and Fe^{3+}-bound forms of Ent, MGE, DGE, and TGE. However, unlike IroD, IroE hydrolyzes *apo* forms more efficiently. The catalytic efficiencies for the *apo* forms are generally about 20-fold higher than those for the Fe^{3+}-bound forms. Furthermore, at higher concentrations, Fe-Ent, Fe-MGE, and Fe-DGE inhibit IroE (Supporting Information). These data suggest that IroE is not the enzyme responsible for iron release from Fe-MGE, Fe-DGE, or Fe-Ent *in vivo*. Therefore, IroD is probably the only enzyme that hydrolyzes Fe-MGE and Fe-DGE to release iron *in vivo*.

Regioselectivity of IroD on *apo* MGE and DGE

As mentioned above, IroD catalyzes the hydrolysis of *apo* MGE and DGE regioselectively, to give a single linear trimer product and a single linear dimer product for each. This regioselectivity is especially interesting given the recently reported structure of micocin E492,[27] in which a linearized MGE is covalently attached the microcin peptide's C-terminus via the C6 hydroxy of the glucose. IroB and IroD homologs are found in the biosynthesis gene cluster of microcin E492 and H47.[28,29] The linearized MGE found in microcin E492 bears the glucosyl exlusively on the DHB-Ser with the free carboxylic acid. Therefore, it would be interesting to determine IroD's regioselectivity and see whether it is similar with the homologs found in the microcin biosynthesis pathway. We performed larger scale MGE and DGE

hydrolysis reactions and isolated the trimer and dimer products in multi-milligram quantities by reverse-phase HPLC purification. Using ^{1}H NMR, ^{13}C NMR, COSY, HSQC, and HMBC experiments (Figure 5 and Supporting Information), we determined the glucose attachment positions in the dimer and trimer products resulting from MGE and DGE hydrolysis. Figure 5A shows the partial HMBC spectra of the trimer from IroD catalyzed MGE hydrolysis, with partial assignments of the ^{1}H and ^{13}C spectra. The assignment of the three sets of α and β protons from the three serine units were based on both COSY and HSQC spectra. The two β protons with lower chemical shifts were assigned to Ser3 with the free hydroxyl group since the β-OH acylated Ser1 and Ser2 β protons should have higher chemical shifts due to the electron-withdrawing properties of the acyl groups. This analysis is confirmed in HMBC spectra because Ser3 β protons are only coupled to the Ser3 carbonyl carbon, while Ser1 and Ser2 β protons are each coupled to two Ser carbonyl carbons. With the assignment of the Ser3 β proton, the rest of the α and β protons, and all the carbonyl carbons, including the DHB carbonyl carbons and the Ser carbonyl carbons, can be assigned by walking through the HMBC spectrum following the ^{2}J and ^{3}J couplings shown in Figure 5A. The DHB1 and DHB3 carbonyl carbon for the trimer appear to have the same chemical shift, and this carbonyl ^{13}C peak is coupled to the C6 proton of the DHB with the glucose attached. Therefore, from this information, we could only conclude that the glucose unit is either on the DHB1 or DHB3, but not on DHB2. Using similar methods, we conclude that in the dimer product arising from MGE hydrolysis, the glucose is attached to DHB1 (Figure 5B). To generate this dimer product requires that the glucose in the trimer product must be attached to DHB1. Therefore, both the trimer and dimer structures from MGE hydrolysis were elucidated as the structures shown in Figure 6. It should be noted that the structure of the linear MGE matches that from microcin E492. The trimer and dimer structures generated by IroD-catalyzed DGE hydrolysis were solved similarly, and the results are summarized in Figure 6.

Interestingly, the dimers generated by IroD-catalyzed DGE hydrolysis and MGE hydrolysis are the same compound, with one glucose on the DHB-Ser with the free carboxylic acid. Careful analysis of the regioselectivity indicates that IroD prefers to hydrolyze the ester bond with glucose attached to the carboxyl-side DHB-Ser unit and no glucose on the hydroxyl-side DHB-Ser unit. If the most favorable ester bond is not present, then IroD will hydrolyze the ester bond with glucose on both DHB-Ser units or no glucose on either DHB-Ser unit, while the ester bond with no glucose on the carboxyl-side DHB-Ser units but with glucose on the hydroxyl-side DHB-Ser unit is least favored (Figure 6).

Discussion

The catecholic siderophore Ent binds Fe^{3+} with a estimated K_d of 10^{-49} M (10^{-35} M at physiological pH). Cyptoplasmic release of Fe^{3+} from such a high affinity complex is generally believed to result from Fes-catalyzed hydrolysis of the trilactone scaffold of Fe-Ent, although reduction of Fe^{3+} to Fe^{2+} might also play a role.[1] The substrate specificity of Fes, however, has been confusing due to conflicting reports[13–16]. We address this issue in the context of this study.

The *iroA* gene cluster from certain pathogenic *E. coli* and *Salmonella* strains encodes two Fes homologs, IroD and IroE, which have been proposed to be glucosylated enterobactin hydrolases based on bioinformatics and genetic studies[17,18]. We have overexpressed and purified all three enzymes, and carried out detailed kinetics studies on both *apo* and Fe^{3+}-bound forms of Ent, MGE, DGE, and TGE. The results provide valuable information about the *in vivo* functions of Fes, IroD, and IroE (summarized in Figure 7).

Fes is the Fe-Ent esterase and it prefers Fe-Ent over *apo* Ent

In the initial activity assay, we found that Fes hydrolyzes *apo* Ent much faster than Fe-Ent, which is consistent with some reports,[16] but not others.[14] Detailed kinetic study indicates that interpreting catalytic turnover (k_{cat}) or the catalytic efficiency (k_{cat}/K_m) yields different conclusions. If Fes is operating at low concentrations of Ent/Fe-Ent in the cytoplasm (which is probably true *in vivo*), the apparent second-order rate constant, k_{cat}/K_m, will be the relevant parameter for measuring throughput. By this criterion, Fes prefers Fe-Ent over *apo* Ent as substrate. The catalytic efficiency is much higher for Fe-Ent (>90 $min^{-1}\mu M^{-1}$) than for *apo* Ent (4 $min^{-1}\mu M^{-1}$). If both Ent and Fe-Ent are present at similar concentrations and the concentration of Fes is limiting, then all nearly all Fes molecules will be bound by Fe-Ent because of its much smaller K_m, and hydrolysis of Fe-Ent will dominate. In this sense, Fe-Ent is a strong inhibitor of *apo* Ent hydrolysis by Fes. Therefore, our results suggest that Fes prefers Fe-Ent over *apo* Ent as the substrate and are consistent with the conclusion that Fes is the Fe-Ent esterase responsible for iron release from Fe-Ent (Figure 7A).

The kinetic data also explain the apparent inconsistency regarding the substrate specificity of Fes (*apo* vs. Fe^{3+}-bound Ent) in the literature.[13–16] The disparate results are likely due to different concentrations of substrates used in the assays. If high concentrations of Fe-Ent and *apo* Ent were used, then the specific activities reported would reflect k_{cat} values and lead to the conclusion that Fes hydrolyzes *apo* Ent more efficiently. In contrast, if low concentrations were used, then the specific activities would reflect k_{cat}/K_m values and lead to the conclusion that Fes hydrolyzes Fe-Ent preferentially. Indeed, in the work of Longman *et al.*,[14] which reports that Fes prefers Fe-Ent as substrate, substrates concentrations of 0.15 μM are used; in contrast, Brickman and McIntosh,[16] who arrive at the opposite conclusion, use substrate concentrations of 750 μM.

IroD is the Fe-MGE/Fe-DGE esterase and it prefers ferric forms over *apo* forms as substrates

The presence of Fes homologs IroD and IroE in the *iroA* cluster suggests that Fes might not be efficient at hydrolyzing Fe-MGE and Fe-DGE for iron release. Our kinetic data indeed show that Fes hydrolyzes Fe-MGE poorly, and does not hydrolyze Fe-DGE or Fe-TGE at all, confirming that IroD, IroE, or both are required for Fe-MGE and Fe-DGE hydrolysis.

Both IroD and IroE catalyze the hydrolysis of *apo* Ent, MGE, DGE, and TGE. However, their activities differ substantially on Fe^{3+}-bound Ent, MGE, DGE, and TGE. IroD hydrolyzes Fe^{3+}-bound forms very efficiently, while IroE hydrolyzes Fe^{3+}-bound forms inefficiently (Table 2). Furthermore, at higher concentrations, Fe^{3+}-bound substrates inhibit the hydrolysis reactions catalyzed by IroE (Supporting Information), while no substrate inhibition was observed for IroD. Therefore, our results suggest that IroD is the Fe-MGE/Fe-DGE esterase responsible for iron release in strains harboring the *iroA* gene cluster(Figure 7B).

Like Fes, IroD prefers the Fe^{3+}-bound form of Ent, MGE, DGE, and TGE as substrates by catalytic efficiency analysis. Even though the absolute k_{cat} values are smaller, the k_{cat}/K_m values for Fe^{3+} bound forms are at least four-fold higher than those for the corresponding *apo* forms, and the K_m values are at least 330-fold lower (Table 2). The low K_m's (~100 nM) of Fes and IroD on Fe^{3+}-bound substrates suggest that the *in vivo* concentrations of these ferric siderophores are also very low.

Even though Fes and IroD also catalyze the hydrolysis of apo siderophores *in vitro*, we do not know whether the activity on apo substrates are physiologically relevant or not. It has been proposed that proteins involved in Ent biosynthesis are membrane-associated and the synthesis of Ent is closely coupled to the export machinery to prevent damage by intracellular *apo* Ent.

[2,30,31] If this is true, it is possible that Fes and IroD do not have access to apo siderophores *in vivo* under normal conditions.

IroD hydrolyzes MGE and DGE regioselectively

IroE hydrolyzes MGE and DGE with little regioselectivity, generating at least two linearized trimer products. In contrast, IroD regioselectively hydrolyzes the trilactone in *apo* MGE and DGE. We have determined the structures of the linearized trimer and dimer products from IroD catalyzed MGE and DGE hydrolysis by NMR. The linear trimer product from MGE hydrolysis is consistent with the linearized MGE structure present in microcin E492,[27] in which the glucose unit is linked to the DHB-Ser that bears the free carboxylic acid group. Therefore, our result agrees with the reported microcin E492 structure and suggests a biosynthetic role for MceD, the IroD homolog found in the microcin E492 gene cluster.[27–29] We could not determine whether the linearized MGE in microcin E492 arises from *apo* MGE hydrolysis or Fe-MGE hydrolysis because HPLC analysis showed that the products from Fe-MGE hydrolysis by IroD are the same as those from *apo* MGE hydrolysis (Supporting Information), suggesting that the regioselectivity is preserved for the hydrolysis of both forms. It is also possible that IroD hydrolyzes MGE after it is attached to the microcin peptide.

The initial hydrolysis of the trilactone scaffold of DGE results in a linear trimer product that has two glucose units which are attached to the DHB-Ser with the free carboxylic acid and to the central DHB-Ser. Interestingly, the linear dimer product from DGE hydrolysis is the same as the dimer product from MGE hydrolysis, with one glucose unit attached to the DHB-Ser bearing the free carboxylic acid. This regioselectivity of IroD can be explained by its preference for Glc-DHB-Ser on the carboxyl-side and DHB-Ser on the hydroxyl-side of the ester bond being hydrolyzed, as illustrated in Figure 6.

The linear trimers and dimers from MGE and DGE hydrolysis by IroD are different from salmochelins S1 and S2,[17] suggesting that salmochelins S1 and S2 detected in *S. enterica* culture broth are probably the products of IroE catalyzed hydrolysis. Since the complete structural characterization of all salmochelins has not been performed, we cannot rule out that IroD also produces ring-opened salmochelins that are subsequently secreted into the culture medium.

IroE hydrolyzes *apo* siderophores more efficiently than Fe^{3+}-bound forms, and *in vivo* probably only works on *apo* forms while they are being exported

IroE was predicted to be a periplasmic protein.[18] The observation that full-length IroE is insoluble while the deletion of the first 30 or 40 amino acids provided soluble IroE supports the prediction that IroE is tethered to the outer leaflet of the cytoplasmic membrane by an N-terminal membrane insertion motif. Our kinetic data suggest that IroE prefers *apo* Ent, MGE, DGE, and TGE as substrates because of its very low catalytic efficiencies for processing the Fe^{3+}-bound forms, and also because it is substrate-inhibited at higher concentrations of Fe-Ent, Fe-MGE, and Fe-DGE. Previous genetic studies indicate that IroE functions *in vivo* because less of the hydrolyzed salmochelins are isolated from bacterial strains harboring the *iroA* cluster lacking *iroE*.[17] These results suggest a model in which IroE acts in the periplasm and hydrolyzes some or all of *apo* Ent, MGE, and DGE while they are being exported out of the cell (Figure 7C). If the inhibition by Fe-Ent, Fe-MGE, Fe-DGE also happens *in vivo*–that is, if IroE has access to Fe-Ent, Fe-MGE and Fe-DGE while they are being imported–then the hydrolysis of *apo* forms would only happen shortly after the cells initiate the synthesis of these siderophores and no Fe^{3+}-bound forms are being imported. However, it is possible that during import, the siderophores are bound to transporter proteins and therefore not accessible to IroE. The fact that bacteria utilize IroE to hydrolyze *apo* siderophores while being exported suggests that the linearized siderophores may behave differently from their macrocyclic counterparts.

In summary, as shown in Figure 7, our in *vitro* study of IroD, IroE and Fes provides important information about their *in vivo* functions and advances our understanding about how bacteria use enterobactin and glucosylated enterobactins as virulence factors to obtain iron from the environment.

Supplementary Material

Refer to Web version on PubMed Central for supplementary material.

Acknowledgements

This work is supported in part by NIH AI 47238 (CTW) and by NIH R01GM065400 (DRL), a postdoctoral fellowship from the Jane Coffin Childs Memorial Fund (HL) and a graduate fellowship from the Hertz Foundation (MAF).

References

1. Raymond KN, Dertz EA, Kim SS. Proc Natl Acad Sci USA 2003;100:3584–3588. [PubMed: 12655062]
2. Crosa JH, Walsh CT. Microbiol Mol Biol Rev 2002;66:223–249. [PubMed: 12040125]
3. Harris WR, Carrano CJ, Cooper SR, Sofen SR, Avdeef AE, McArdle JV, Raymond KN. J Am Chem Soc 1979;101:6097–6104.
4. Loomis LD, Raymond KN. Inorg Chem 1991;30:906.
5. Gehring AM, Bradley KA, Walsh CT. Biochemistry 1997;36:8495–8503. [PubMed: 9214294]
6. Gehring AM, Mori I, Walsh CT. Biochemistry 1998;37:2648–2659. [PubMed: 9485415]
7. Shaw-Reid CA, Kelleher NL, Losey HC, Gehring AM, Berg C, Walsh CT. Chem Biol 1999;6:385–400. [PubMed: 10375542]
8. Ehmann DE, Shaw-Reid CA, Losey HC, Walsh CT. Proc Natl Acad Sci USA 2000;97:2509–2514. [PubMed: 10688898]
9. Finking R, Marahiel MA. Annu Rev Microbiol 2004;58:453–488. [PubMed: 15487945]
10. Furrer JL, Sanders DN, Hook-Barnard IG, McIntosh MA. Mol Microbiol 2002;44:1225–1234. [PubMed: 12068807]
11. Faraldo-Gómez JD, Sansom MSP. Nat Rev Mol Cell Biol 2003;4:105–116. [PubMed: 12563288]
12. Braun V, Braun M. Curr Opin Microbiol 2002;5:194–201. [PubMed: 11934617]
13. Bryce GF, Brot N. Biochemistry 1972;11:1708–1715. [PubMed: 4337557]
14. Langman L, Young IG, Frost GE, Rosenberg H, Gibson F. J Bacteriol 1972;112:1142–1149. [PubMed: 4565531]
15. Greenwood KT, Luke RKJ. Biochim Biophys Acta 1978;525:209–218. [PubMed: 150859]
16. Brickman TJ, McIntosh MA. J Biol Chem 1992;267:12350–12355. [PubMed: 1534808]
17. Bister B, Bischoff D, Nicholson GJ, Valdebenito M, Schneider K, Winkelmann G, Hantke K, Sussmuth RD. Biometals 2004;17:471–481. [PubMed: 15259369]
18. Hantke K, Nicholson G, Rabsch W, Winkelmann G. Proc Natl Acad Sci USA 2003;100:3677–3682. [PubMed: 12655053]
19. Goetz DH, Holmes MA, Borregaard N, Bluhm ME, Raymond KN, Strong RK. Mol Cell 2002;10:1033–1043. [PubMed: 12453412]
20. Flo TH, Smith KD, Sato S, Rodriguez DJ, Holmes MA, Strong RK, Akira S, Aderem A. Nature 2004;432:917–921. [PubMed: 15531878]
21. Baumler AJ, Norris TL, Lasco T, Voight W, Reissbrodt R, Rabsch W, Heffron F. J Bacteriol 1998;180:1446–1453. [PubMed: 9515912]
22. Rabsch W, Methner U, Voigt W, Tschape H, Reissbrodt R, Williams PH. Infect Immun 2003;71:6953–6961. [PubMed: 14638784]
23. Baumler AJ, Tsolis RM, Velden AWMvd, Stojiljkovic I, Anic S, Heffron F. Gene 1996;183:207–213. [PubMed: 8996108]

24. Fischbach MA, Lin H, Liu DR, Walsh CT. Proc Natl Acad Sci USA 2005;102:571–576. [PubMed: 15598734]
25. Ramirez RJA, Karamanukyan L, Ortiz S, Gutierrez CG. Tetrahedron Lett 1997;38:749–752.
26. Corey EJ, Bhattacharyya S. Tetrahedron Lett 1977;45:3919–3922.
27. Thomas X, Destoumieux-Garzon D, Peduzzi J, Afonso C, Blond A, Birlirakis N, Goulard C, Dubost L, Thai R, Tabet JC, Rebuffat S. J Biol Chem 2004;279:28233–28242. [PubMed: 15102848]
28. Azpiroz MF, Lavina M. Antimicrob Agents Chemother 2004;48:1235–1241. [PubMed: 15047525]
29. Corsini G, Baeza M, Monasterio O, Lagos R. Biochimie 2002;84:539–544. [PubMed: 12423798]
30. Hantash FM, Earhart CF. J Bacteriol 2000;182:1768–1773. [PubMed: 10692387]
31. Armstrong SK, Pettis GS, Forrester LJ, McIntosh MA. Mol Microbiol 1989;3:757–766. [PubMed: 2526281]

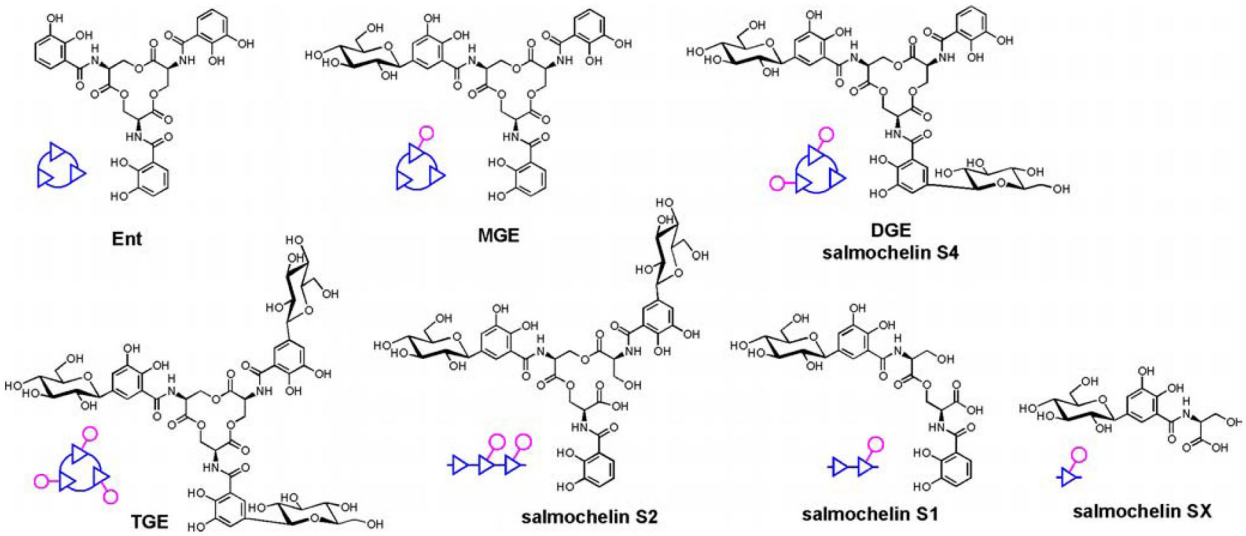

Figure 1.
Structures of enterobactin, glucosylated enterobactins, and some of their degradation products. Next to each structure is a schematic representation of the compound, where a blue triangle represents DHB-Ser, and a pink circle represents glucose. Similar schematic representations are used in subsequent figures.

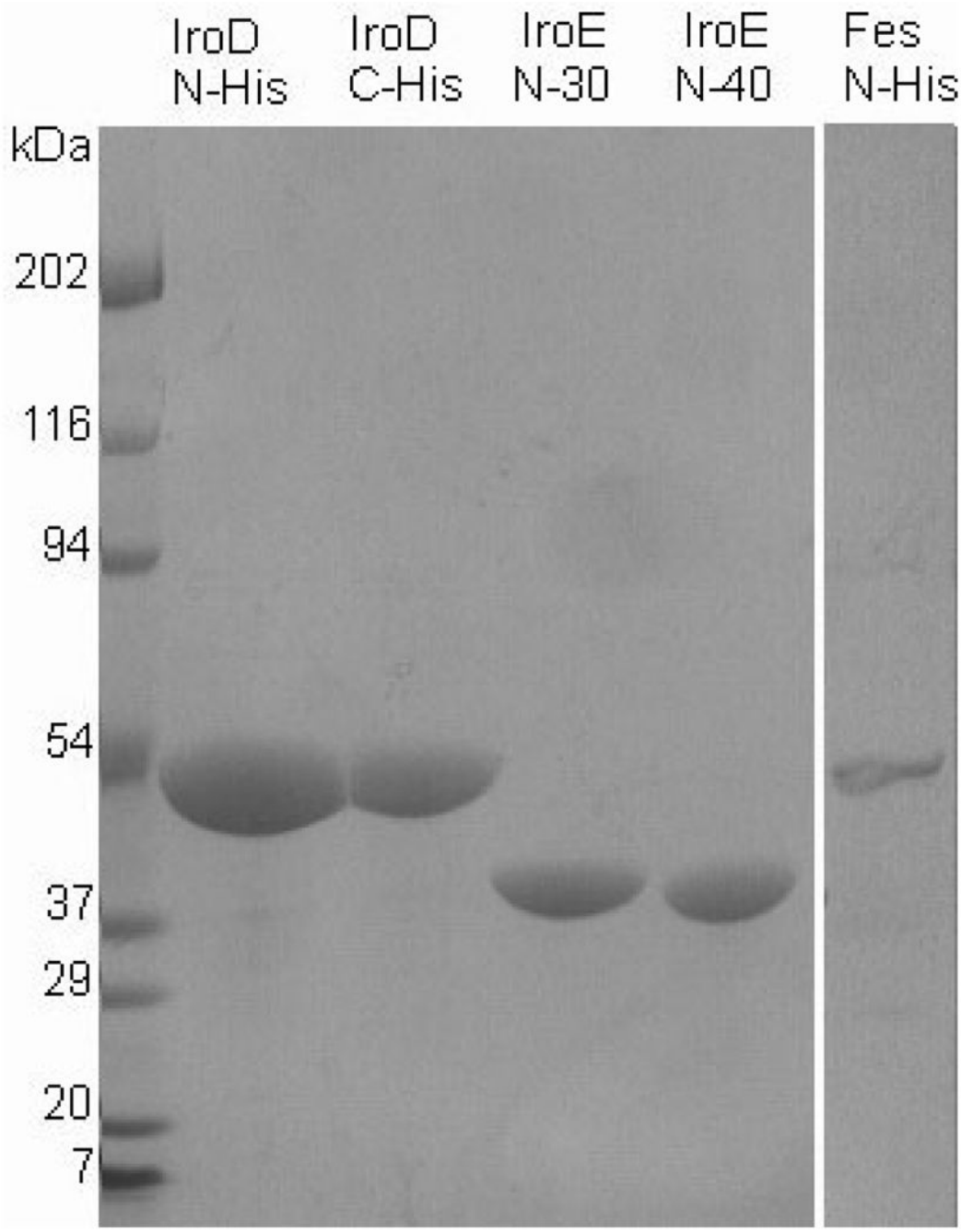

Figure 2.
SDS/PAGE analysis of purified IroD (with either N- or C-terminal His_6 tag), IroE (N-terminal 30 aa or 40 aa deletion, with C-terminal His_6 tag), and Fes (with N-terminal His_6 tag).

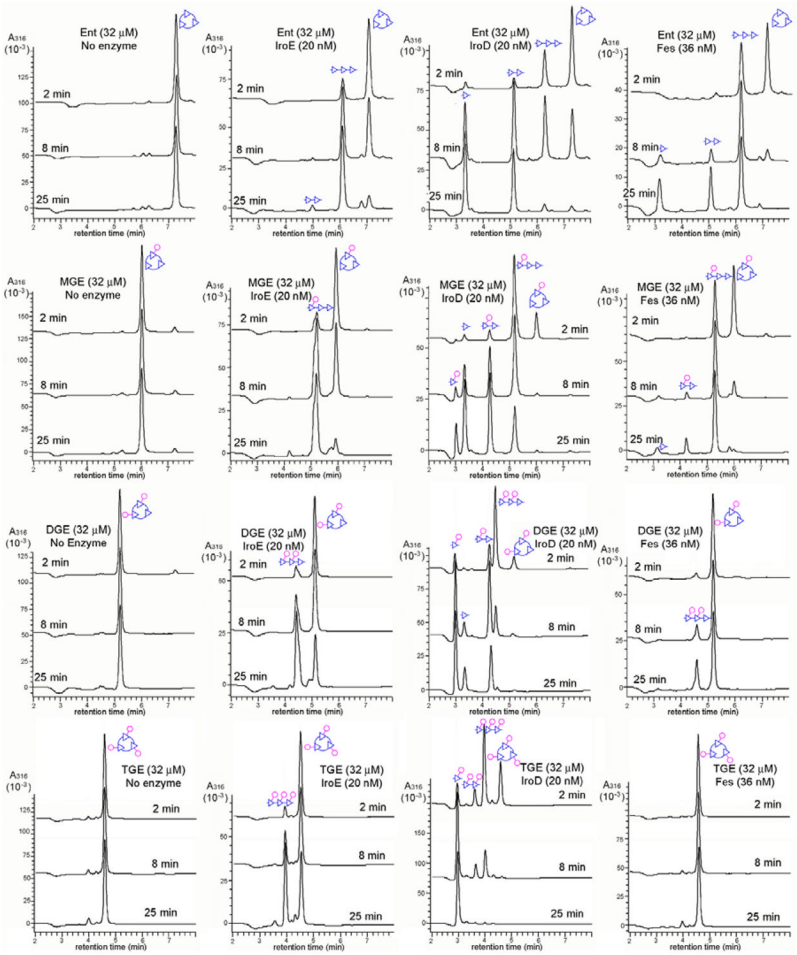

Figure 3.

Reaction time courses of IroE, IroD, and Fes-catalyzed hydrolysis of *apo* Ent, MGE, DGE, and TGE. Reaction aliquots were quenched at different time points and analyzed by LC/MS. The assignment of the hydrolysis products is based on the MS data, and the schematic representations of the hydrolysis products are shown. For the linear trimer and dimer products from MGE and DGE hydrolysis, the schematic representation of only one possible regioisomer is shown.

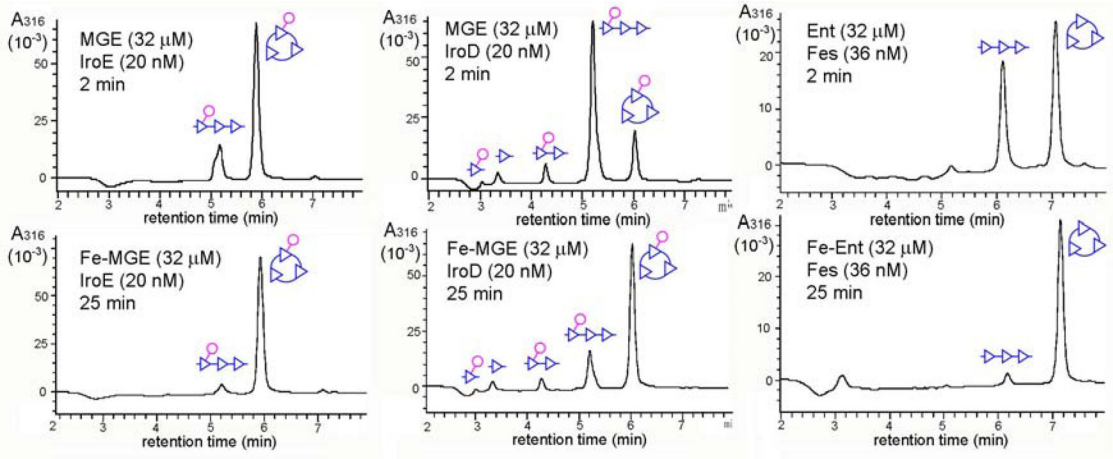

Figure 4.

IroE, IroD and Fes catalyze the hydrolysis of Fe^{3+}-bound forms of Ent, MGE, DGE, and TGE more slowly than the *apo* forms under the same conditions used. IroE and IroD catalyzed hydrolysis of MGE vs. Fe-MGE, Fes catalyzed hydrolysis of Ent vs. Fe-Ent are shown for comparison.

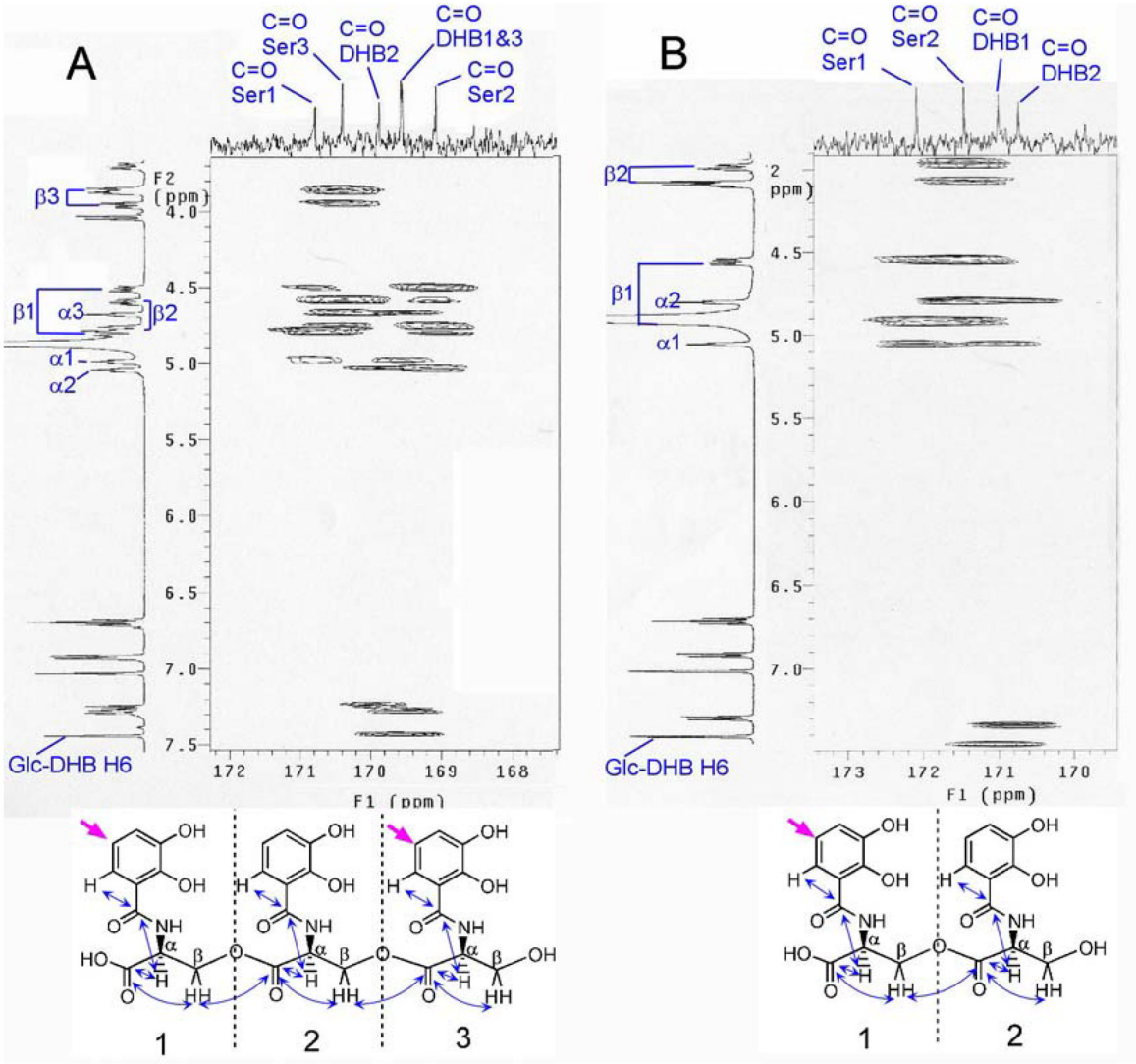

Figure 5.

Partial HMBC spectra of MGE linear trimer (A) and dimer (B) obtained from IroD-catalyzed hydrolysis reaction. Partial assignments are shown, which are based on HSQC, COSY, and HMBC. The pink arrows indicate possible glucose attachment sites. The blue arrows indicate carbon-proton ^{2}J and ^{3}J couplings present in the molecules that are used to determine the structures.

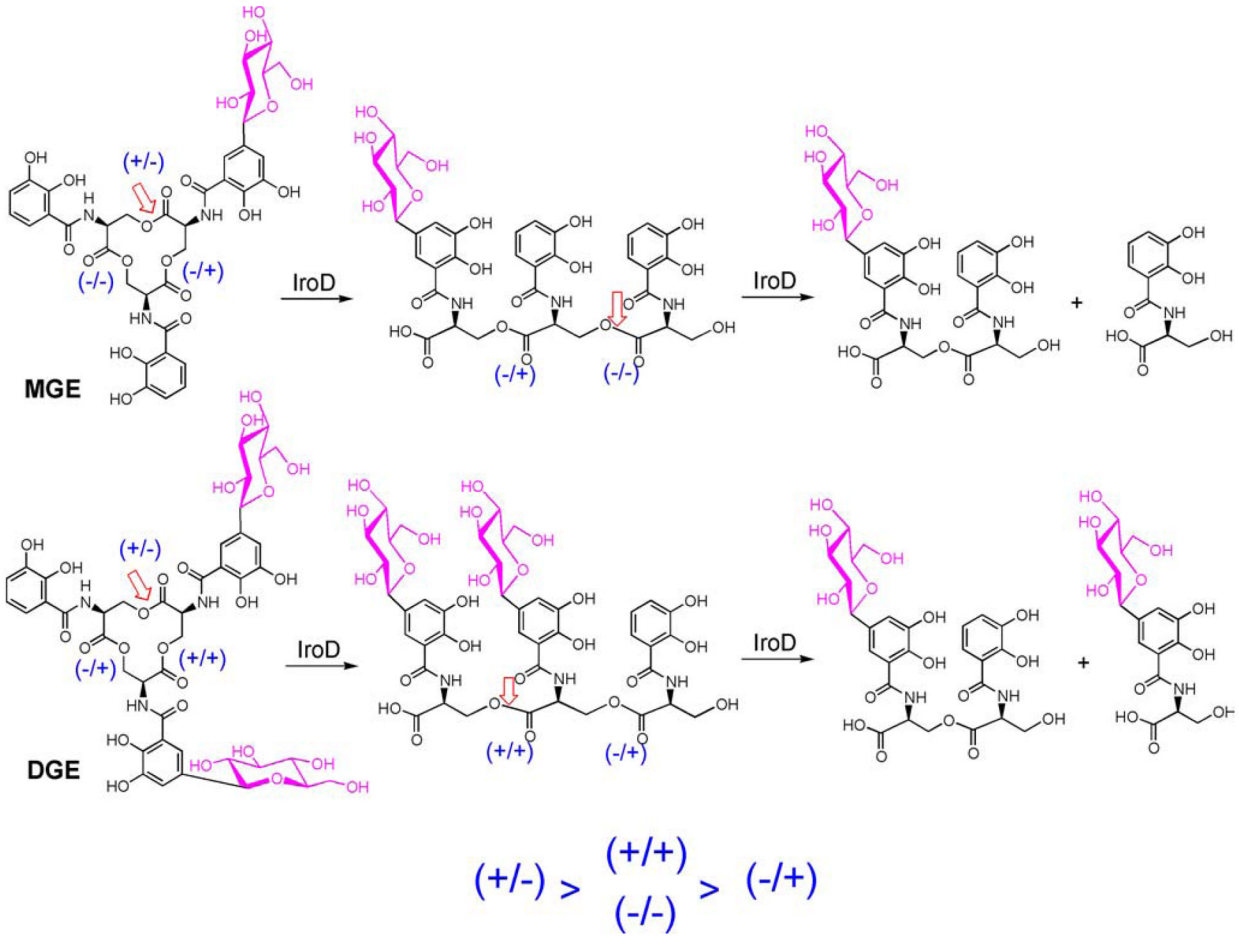

Figure 6.

Summary of IroD regioselectivity on intact macrolactones and linear trimers. The structures of the linear trimers and dimer from IroD catalyzed hydrolysis of MGE and DGE are shown, with the preferred hydrolysis site indicated at each step. The regioselectivity of IroD can be generalized from these results. Based on the presence (+) or absence (−) of glucose on the carboxyl-side DHB ring and the hydroxyl-side DHB ring, each ester bond can be characterized with one of the following symbols, (+/+), (+/−), (−/+), and (−/−). The first '+' or '−' sign indicates the presence or absence of glucose on the carboxyl-side DHB ring, while the second sign indicates the presence or absence of glucose on the hydroxyl-side DHB ring. The order of IroD preference is (+/−) > (+/+), (−/−) > (−/+) for the hydrolysis of intact macrolactones and linear trimers.

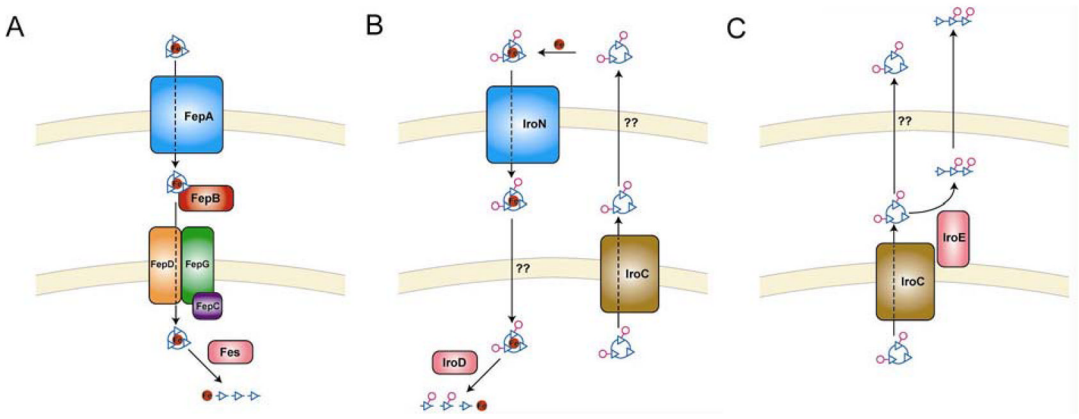

Figure 7.
A schematic representation showing the possible functions of Fes, IroD, and IroE.

Table 1

MS *m/z* data for *apo* Ent, MGE, DGE, and TGE hydrolysis product by IroD, IroE, and Fes. Product distribution for different enzymes/substrates is shown in Figure 3.

	Ent	MGE	DGE	TGE
m/z calc. macrolactone (M^+)	669.1	831.2	993.3	1155.3
m/z obs.	669.6	831.6	993.9	1155.4
m/z calc. linear trimer (M^+)	687.1	849.2	1011.3	1173.3
m/z obs.	687.4	849.9	1011.5	1173.2
m/z calc. Linear dimmer (M^+)	464.1	626.2	626.2	788.2
m/z obs.	464.9	626.7	626.8	788.8
m/z calc. monomer (M^+)	241.1	241.1	241.1	NA
m/z obs.*	240.1	240.1	240.1	NA
m/z calc. monomer(with Glc) (M^+)	NA	403.1	403.1	403.1
m/z obs.	NA	404.1	404.1	403.8

* Detected with negative ion mode. All others were detected with positive ion mode.

J Am Chem Soc. Author manuscript; available in PMC 2008 September 15.

Table 2

Kinetics data of Fes, IroD, and IroE.

		Ent	Fe-Ent	MGE	Fe-MGE	DGE	Fe-DGE	TGE	Fe-TGE
Fes	k_{cat} (min^{-1})	>520[a]	9 ± 1	850 ± 65	1.4 ± 0.1	>78[a]	NA	NA	NA
	K_m (μM)	>130[a]	<0.1[b]	100 ±15	0.29 ± 0.05	>130[a]	NA	NA	NA
	k_{cat}/K_m ($min^{-1}\mu M^{-1}$)	4.0	>90	8.5	4.8	0.6	NA	NA	NA
IroD	k_{cat} (min^{-1})	1060 ± 60	74 ± 4	3720 ± 360	46 ± 2	6500 ± 540	32 ± 2	4460 ± 470	84 ± 2
	K_m (μM)	40 ± 5	0.12 ± 0.04	60 ± 15	0.08 ± 0.02	120 ± 20	0.12 ± 0.2	160 ± 30	0.43 ± 0.04
	k_{cat}/K_m ($min^{-1}\mu M^{-1}$)	26	617	62	575	54	267	28	195
IroE[c]	k_{cat} (min^{-1})	375 ± 40	3.0 ± 0.1	430 ± 10	3.2 ± 0.3	320 ± 20	2.5 ± 0.3	450 ± 30	>8[a]
	K_m (μM)	16 ± 4	3.4 ± 0.2	29 ± 2	4.8 ± 0.7	39 ± 6	4.6 ± 1.0	155 ± 30	>16[a]
	k_{cat}/K_m ($min^{-1}\mu M^{-1}$)	23	0.9	14	0.7	8	0.5	3	0.5

[a] cannot be determined because no saturation was observed up to the highest concentrations tested..

[b] cannot be determined because saturation was reached even at the lowest concentration (0.125 μM) used.

[c] at higher concentrations of Fe-Ent, Fe-MGE, and Fe-TGE, IroE was substrate inhibited.

J Am Chem Soc. Author manuscript; available in PMC 2008 September 15.